Supporting Information

for

New Phosphonite Ligands with High Steric Demand and Low Basicity: Synthesis, Structural Properties, and Cyclometalated Complexes of Pt(II).

María M. Alcaide [1], Matteo Pugliesi [2], Eleuterio Álvarez [1], Joaquín López-Serrano [1,*] and Riccardo Peloso [1,*]

[1] Instituto de Investigaciones Químicas (IIQ), Departamento de Química Inorgánica and Centro de Innovación en Química Avanzada (ORFEO–CINQA), Consejo Superior de Investigaciones Científicas (CSIC) and Universidad de Sevilla, 41092 Sevilla, Spain.
[2] Departimento di Chimica e Chimica Industriale, Universitá di Pisa, Via G. Moruzzi 13, I-56124 Pisa, Italy.

* Correspondence: rpeloso@us.es

Table S1. Crystal data and structure refinement for compound **1·CO**

Empirical formula	$C_{36}H_{31}N_2O_7PPt$
Formula weight	829.69
Temperature	193(2) K
Wavelength	0.71073 Å
Crystal system	Monoclinic
Space group	C2/c
Unit cell dimensions	a = 19.2942(3) Å $\quad$ α= 90°.
	b = 13.1677(3) Å $\quad$ β= 109.9290(10)°.
	c = 27.7585(6) Å $\quad$ γ = 90°.
Volume	6630.0(2) Å^3
Z	8
Density (calculated)	1.662 Mg/m^3
Absorption coefficient	4.333 mm^{-1}
F(000)	3280
Crystal size	0.400 x 0.300 x 0.200 mm^3
Theta range for data collection	1.911 to 30.517°.
Index ranges	-26<=h<=27, -18<=k<=17, -39<=l<=39
Reflections collected	43363
Independent reflections	10110 [R(int) = 0.0286]
Completeness to theta = 25.242°	99.9 %
Absorption correction	Semi-empirical from equivalents
Max. and min. transmission	0.7461 and 0.4425
Refinement method	Full-matrix least-squares on F^2
Data / restraints / parameters	10110 / 42 / 429
Goodness-of-fit on F^2	0.996
Final R indices [I>2sigma(I)]	R1 = 0.0210, wR2 = 0.0490
R indices (all data)	R1 = 0.0257, wR2 = 0.0513
Extinction coefficient	n/a
Largest diff. peak and hole	1.124 and -0.865 e.Å^{-3}

Table S2. Crystal data and structure refinement for compound **2**.

Empirical formula	$C_{70}H_{60}Cl_6N_4O_{12}P_2Pt_2$
	[$C_{68}H_{56}Cl_2N_4O_{12}P_2Pt_2$, 2($CH_2Cl_2$)]
Formula weight	1814.04
Temperature	293(2) K
Wavelength	0.71073 Å
Crystal system	Monoclinic
Space group	I2
Unit cell dimensions	a = 16.1829(14) Å $\alpha = 90°$.
	b = 12.6047(10) Å $\beta = 102.259(3)°$.
	c = 17.6419(15) Å $\gamma = 90°$.
Volume	3516.5(5) $Å^3$
Z	2
Density (calculated)	1.713 Mg/m^3
Absorption coefficient	4.311 mm^{-1}
F(000)	1784
Crystal size	0.50 x 0.40 x 0.20 mm^3
Theta range for data collection	2.066 to 30.562°.
Index ranges	-22<=h<=23, -17<=k<=18, -25<=l<=25
Reflections collected	37774
Independent reflections	10533 [R(int) = 0.0335]
Completeness to theta = 25.242°	99.9 %
Absorption correction	Semi-empirical from equivalents
Max. and min. transmission	0.7461 and 0.3665
Refinement method	Full-matrix least-squares on F^2
Data / restraints / parameters	10533 / 31 / 438
Goodness-of-fit on F^2	0.998
Final R indices [I>2sigma(I)]	R1 = 0.0241, wR2 = 0.0642
R indices (all data)	R1 = 0.0248, wR2 = 0.0651
Absolute structure parameter	0.017(7)
Extinction coefficient	n/a
Largest diff. peak and hole	0.883 and -2.360 e.$Å^{-3}$

Table S3. Crystal data and structure refinement for compound **3·SMe2**.

Empirical formula	$C_{40}H_{41}N_2O_6PPtS$
Formula weight	903.87
Temperature	298(2) K
Wavelength	0.71073 Å
Crystal system	Monoclinic
Space group	$P2_1/c$
Unit cell dimensions	$a = 16.041(6)$ Å $\quad \alpha = 90°$.
	$b = 11.559(5)$ Å $\quad \beta = 108.731(14)°$.
	$c = 21.563(8)$ Å $\quad \gamma = 90°$.
Volume	$3787(3)$ Å^3
Z	4
Density (calculated)	1.585 Mg/m^3
Absorption coefficient	3.852 mm^{-1}
F(000)	1808
Crystal size	$0.400 \times 0.300 \times 0.200$ mm^3
Theta range for data collection	1.995 to 30.559°.
Index ranges	$-22 \le h \le 22$, $-16 \le k \le 15$, $-30 \le l \le 30$
Reflections collected	129299
Independent reflections	11541 [R(int) = 0.0405]
Completeness to theta = 25.242°	99.8 %
Absorption correction	Semi-empirical from equivalents
Max. and min. transmission	0.7461 and 0.4801
Refinement method	Full-matrix least-squares on F^2
Data / restraints / parameters	11541 / 276 / 468
Goodness-of-fit on F^2	1.042
Final R indices [I>2sigma(I)]	R1 = 0.0258, wR2 = 0.0673
R indices (all data)	R1 = 0.0334, wR2 = 0.0728
Extinction coefficient	n/a
Largest diff. peak and hole	1.595 and -1.922

Additional comments on conformational analyses

We have performed relaxed potential energy scans of the rotation around the P—C bond of **PAr^{Xyl2}(OPh^{NO2})$_2$** and **PAr^{Xyl2}(OPh^{NO2,Me})$_2$** at the same level of theory as the geometry optimizations. Also, we have performed full conformational analysis using semiempirical quantum mechanical methods (GFNn–xTB) and the CREST code [1,2]. Analysis of these results confirm the calculated geometries discussed in the main text as the most stable type of conformer for each ligand, even though in the case of **PAr^{Xyl2}(OPh^{NO2})$_2$** conformations B and C are almost degenerate. In addition, the relaxed scan calculations suggest that P—C rotation is facile for both ligands (almost barrierless for **PAr^{Xyl2}(OPh^{NO2})$_2$**).

[1] Pracht, P.; Bohle, F.; Grimme, S. Automated exploration of the low-energy chemical space with fast quantum chemical methods. *Phys. Chem. Chem. Phys.* **2020**, *22*, 7169-7192.

[2] Grimme, S. Exploration of Chemical Compound, Conformer, and Reaction Space with Meta-Dynamics Simulations Based on Tight-Binding Quantum Chemical Calculations. *J. Chem. Theory Comput.* **2019**, *15*, 2847-2862.

NMR spectra
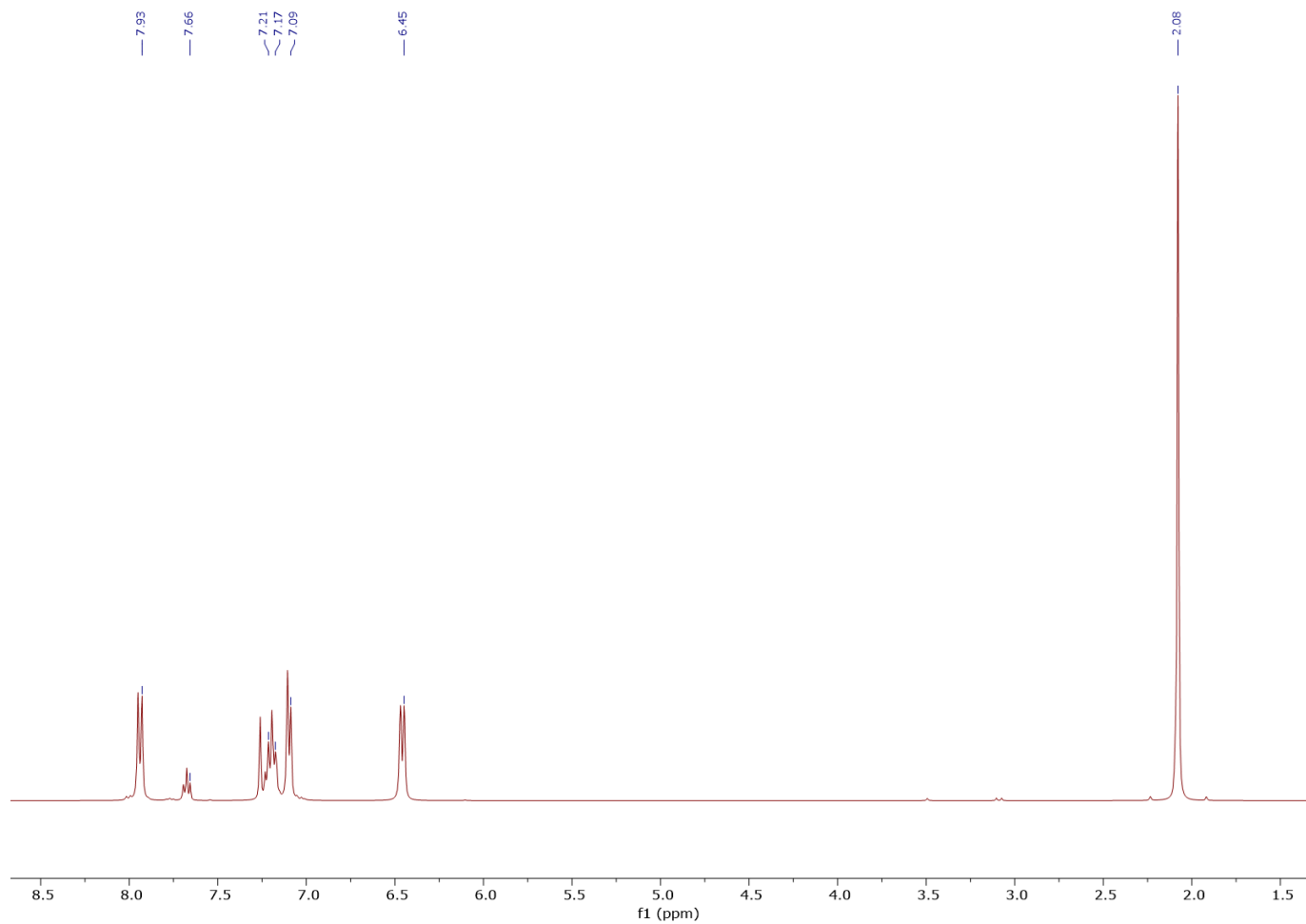
Figura S1. ^{1}H NMR spectrum of **PAr^{Xyl2}(OPh^{NO_2})$_2$** in CDCl$_3$.
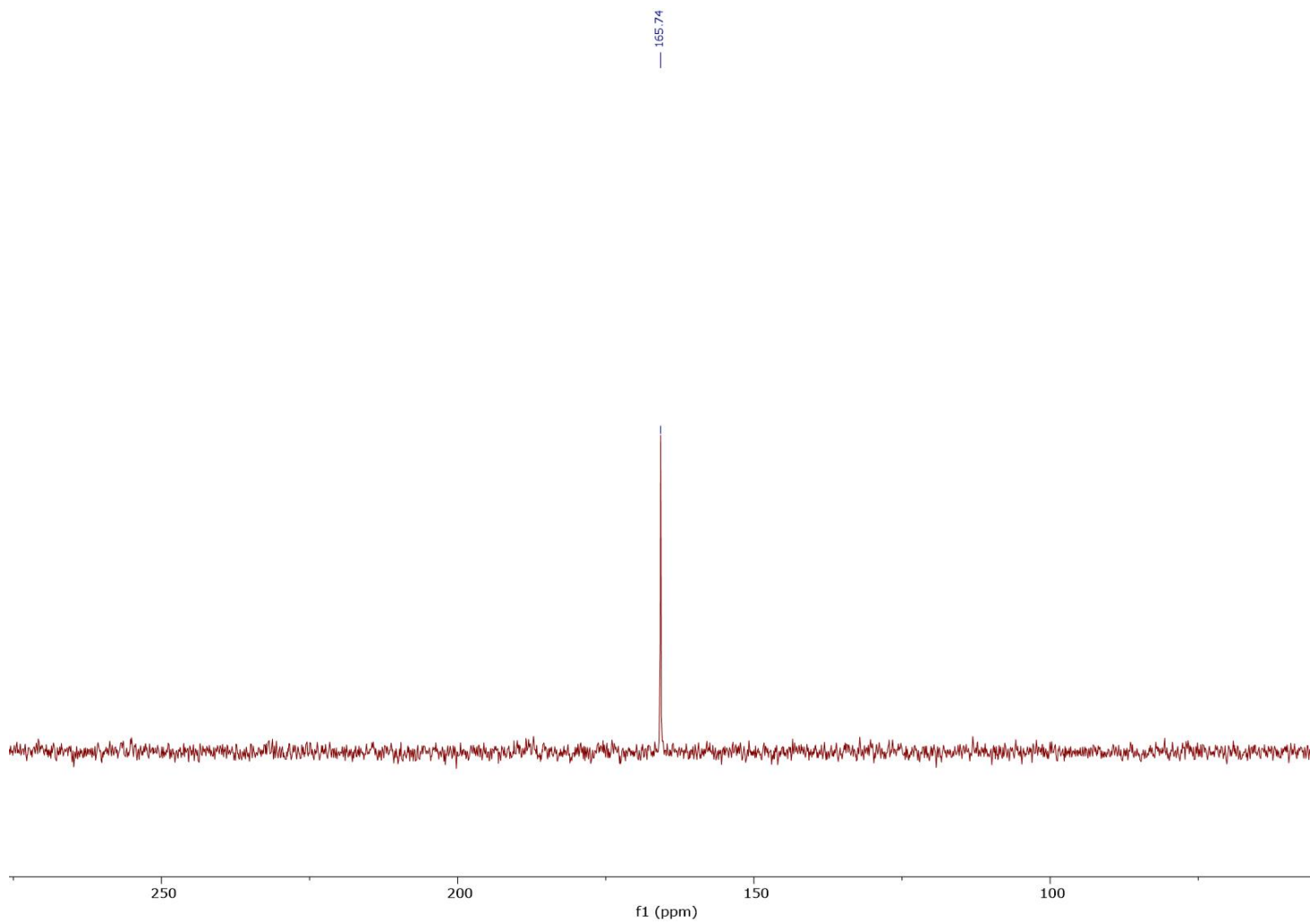
Figura S2. $^{31}P\{^1H\}$ NMR spectrum of complx of **PAr^{Xyl2}(OPh^{NO_2})$_2$** in CDCl$_3$.
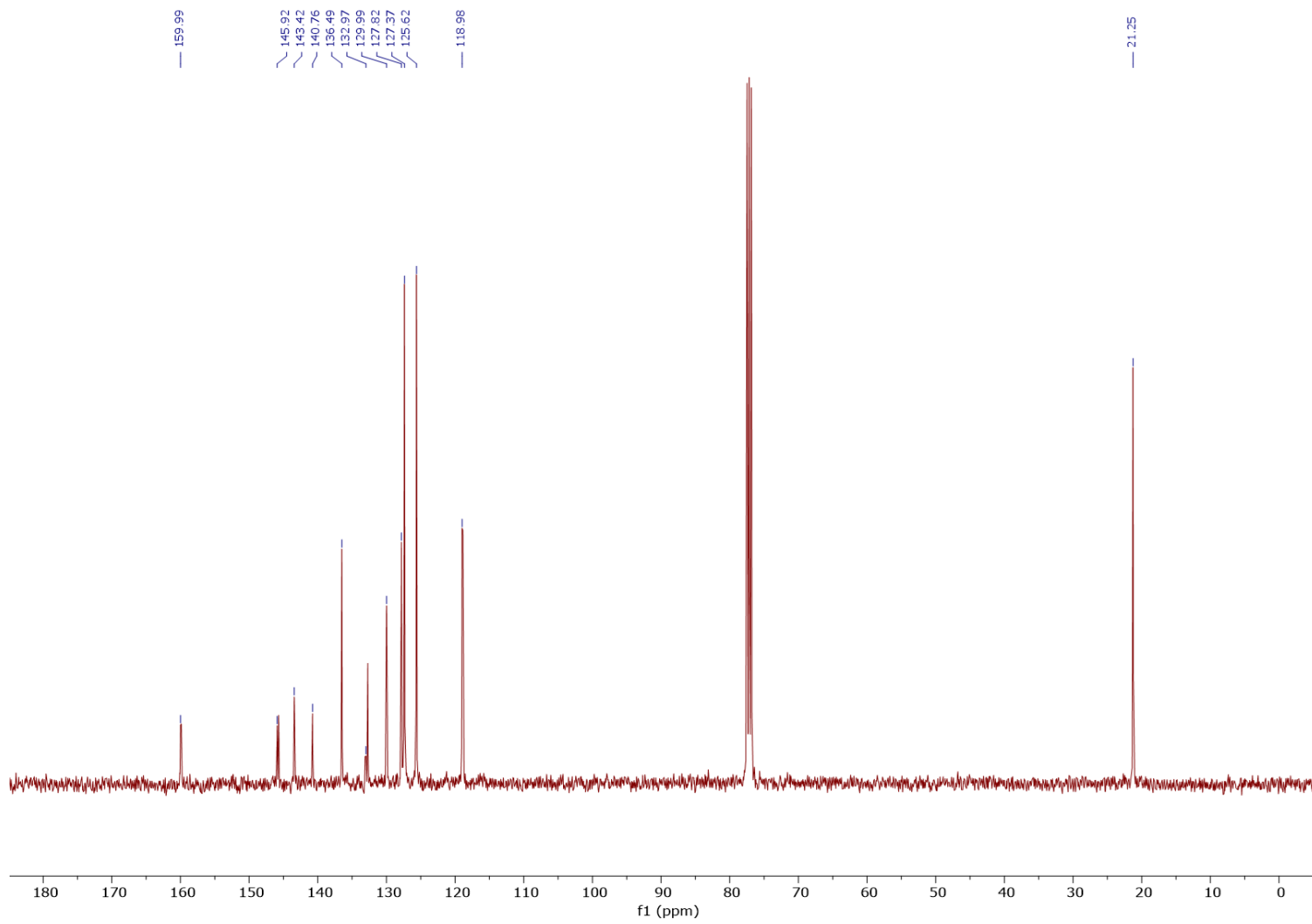
Figura S3. $^{13}C\{^{1}H\}$ NMR spectrum of **PAr^{Xyl2}(OPh^{NO2})$_2$** in CDCl$_3$.
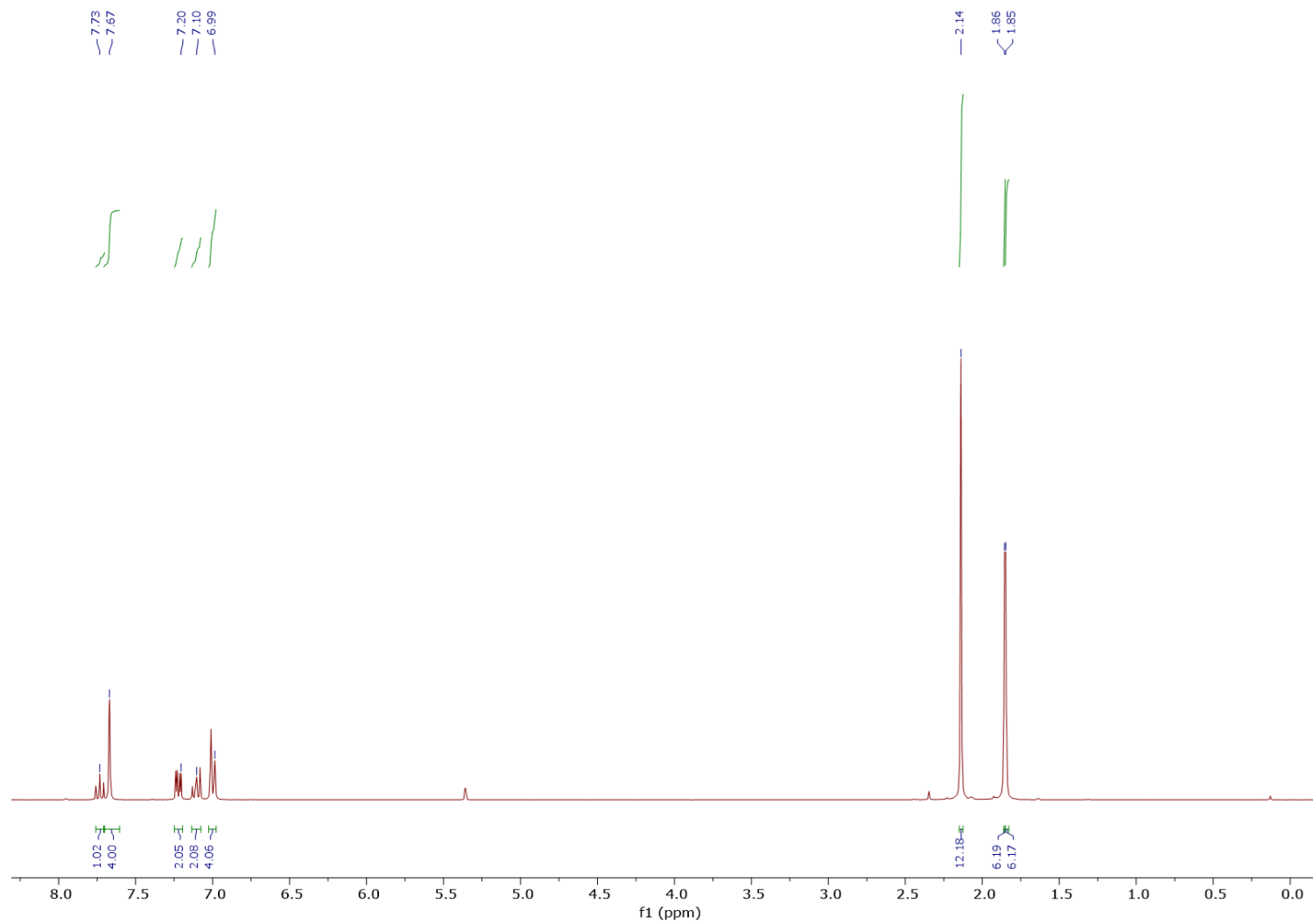
Figura S4. ^{1}H NMR spectrum of complex of **PAr^{Xyl2}(OPh^{NO_2,Me})$_2$** in CD$_2$Cl$_2$.
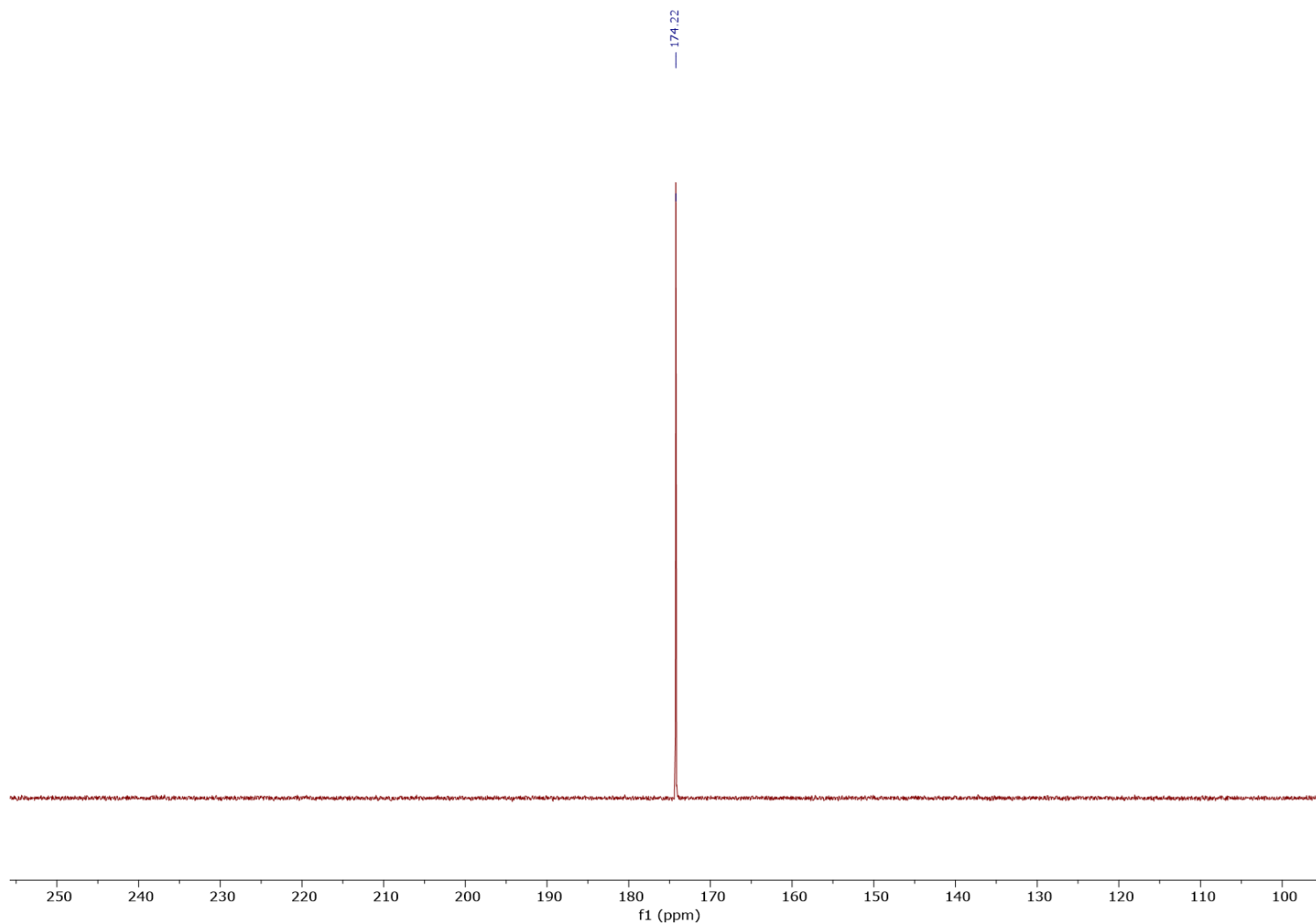
Figura S5. $^{31}P\{^{1}H\}$ NMR spectrum of complex of $PAr^{Xyl2}(OPh^{NO_2,Me})_2$ in CD_2Cl_2.
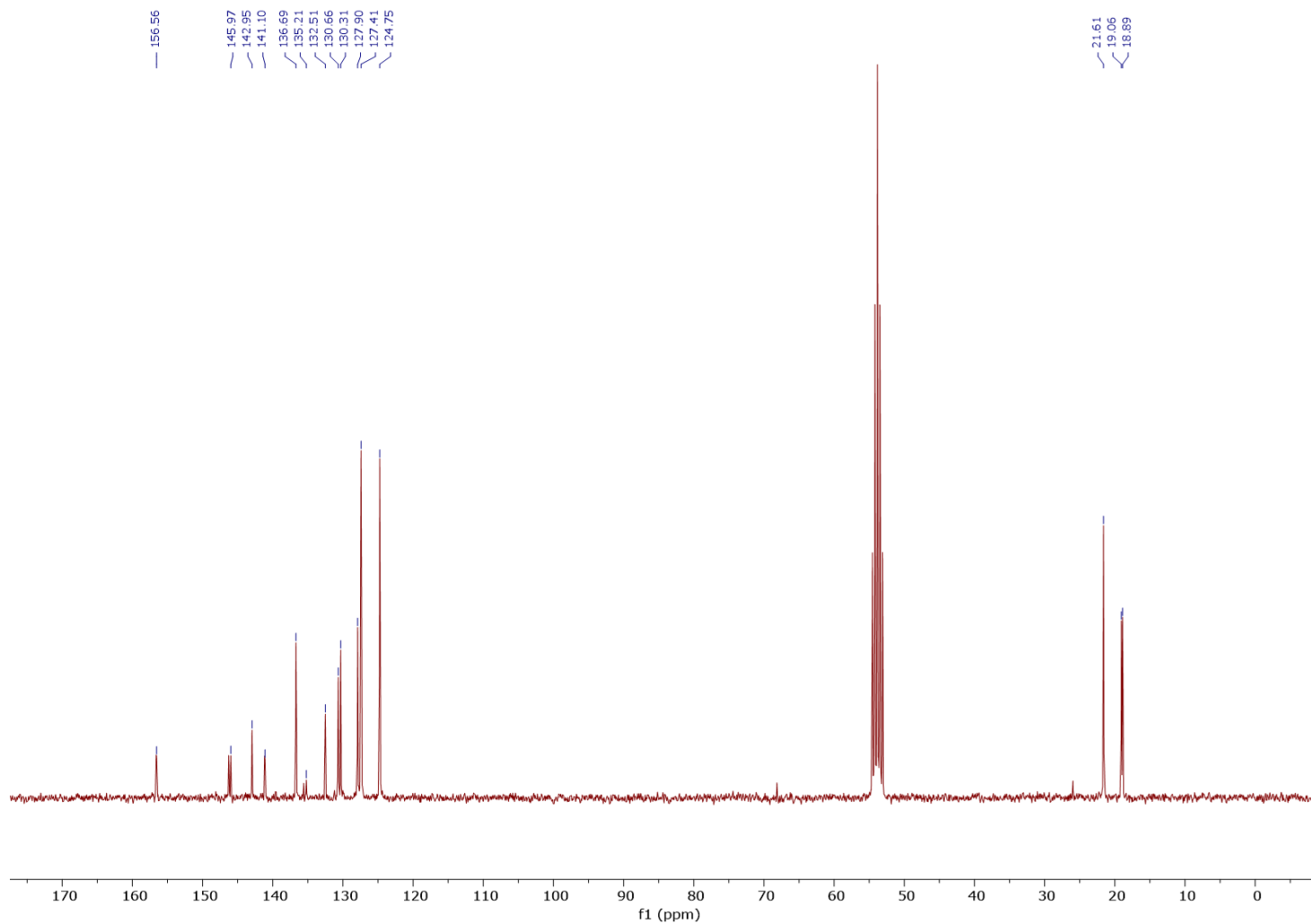
Figura S6. $^{13}C\{^1H\}$ NMR spectrum of complex of **PAr^{Xyl2}(OPh^{NO_2,Me})$_2$** in CD$_2$Cl$_2$.
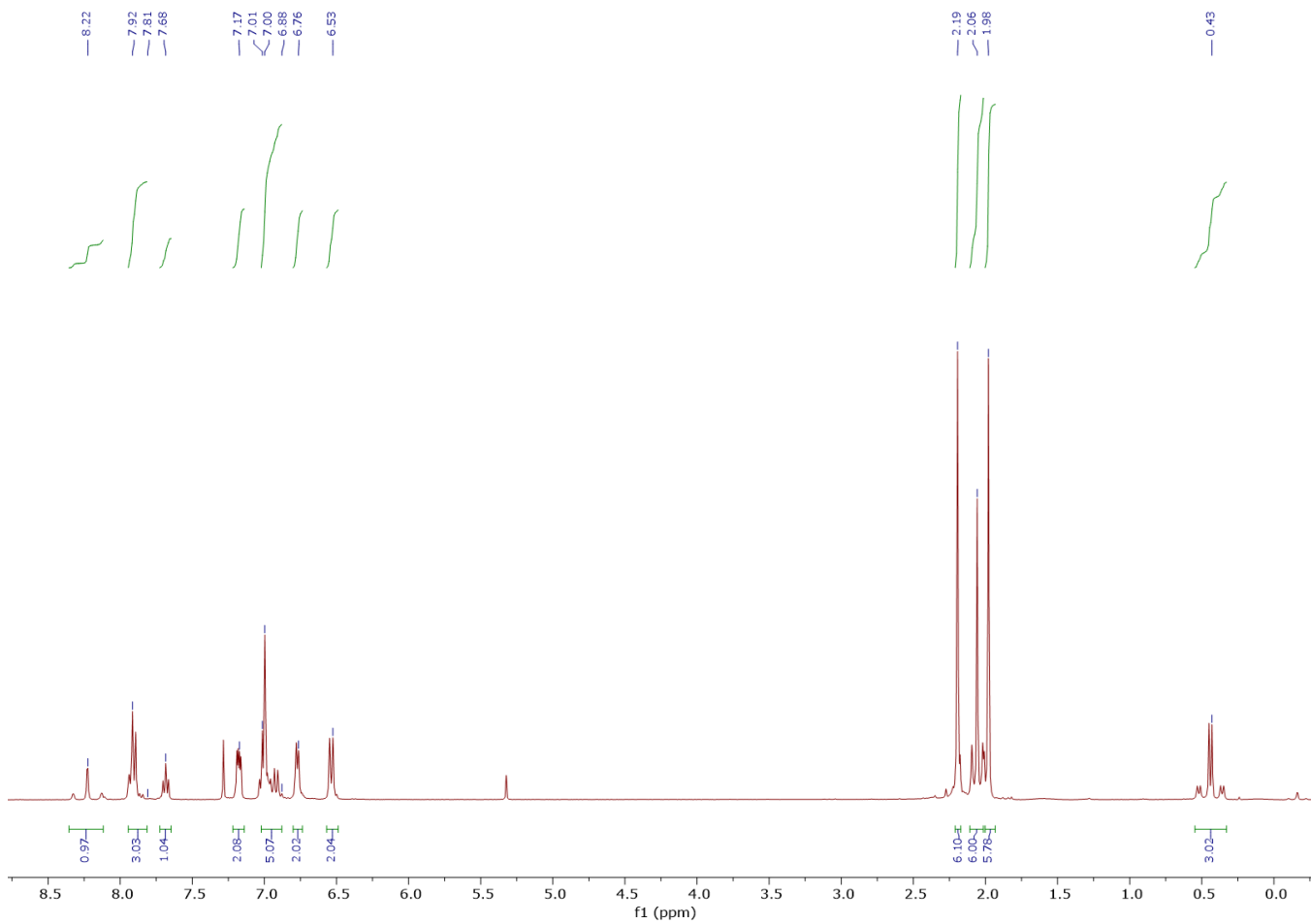
Figura S7. ^{1}H NMR spectrum of complex of **1·SMe$_2$** in CD$_2$Cl$_2$.

169.33

f1 (ppm)
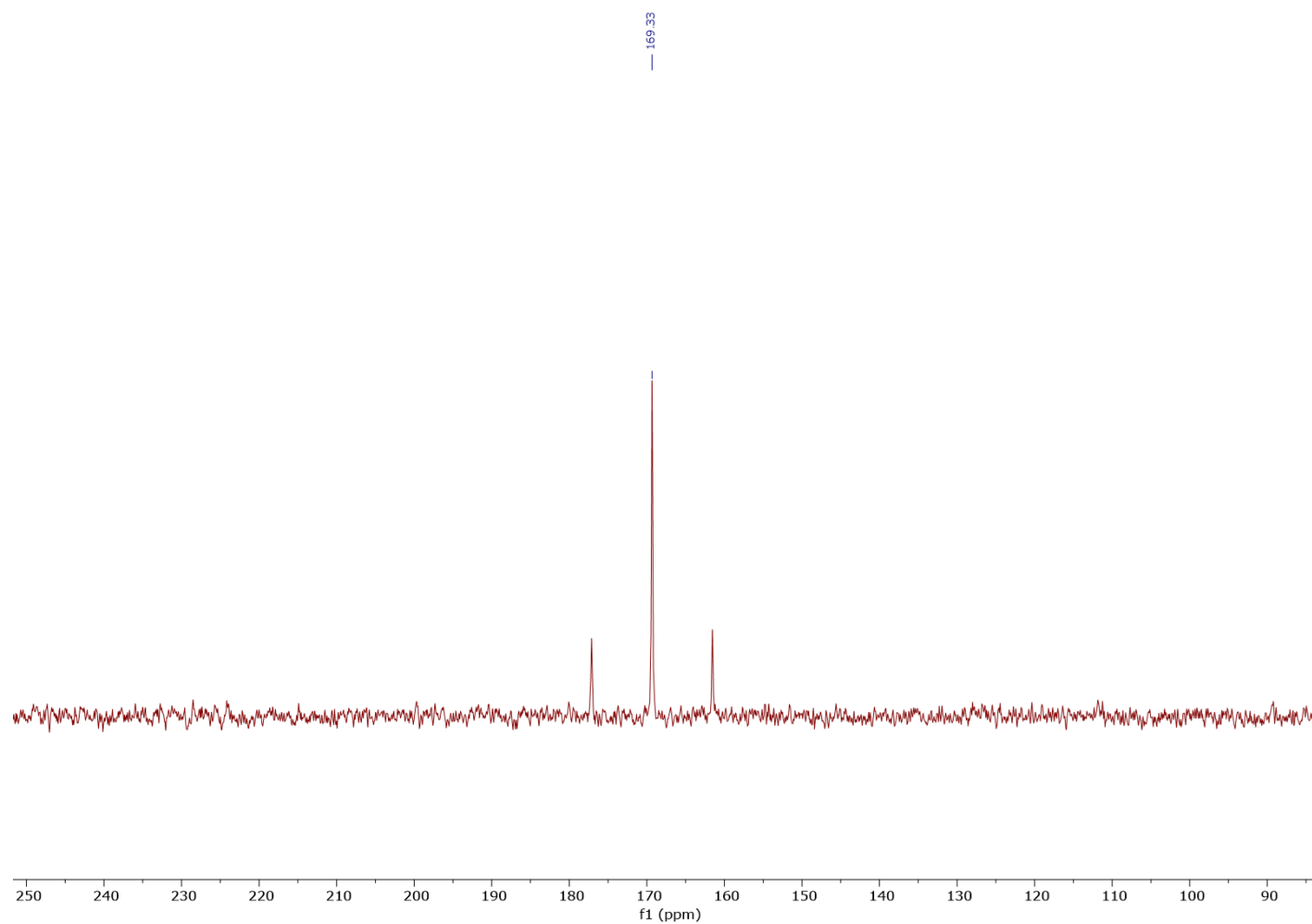
Figura S8. $^{31}P\{^{1}H\}$ NMR spectrum of complex of **1·SMe₂** in CD₂Cl₂.
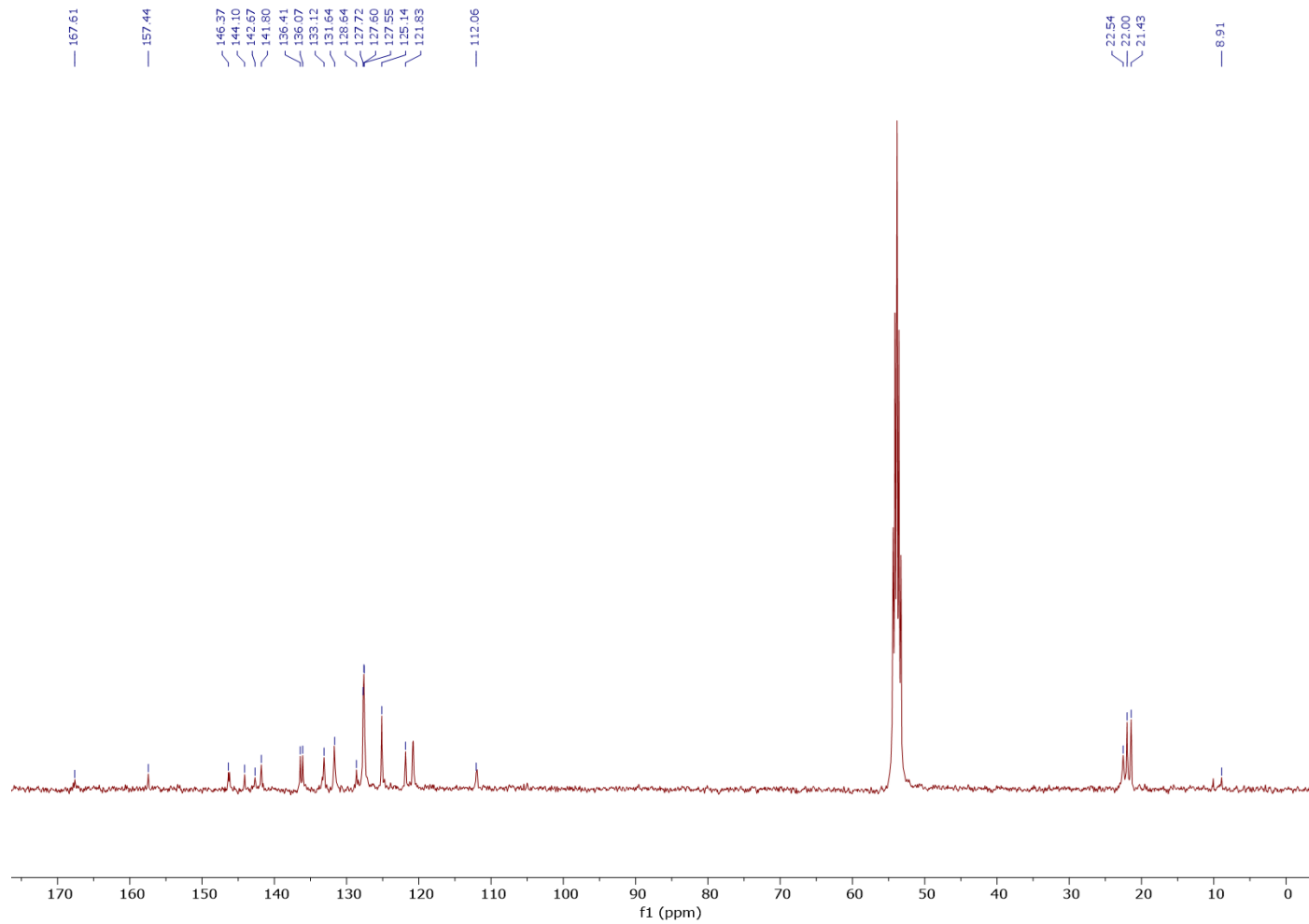
Figura S9. $^{13}C\{^{1}H\}$ NMR spectrum of complex of **1·SMe₂** in CD_2Cl_2.
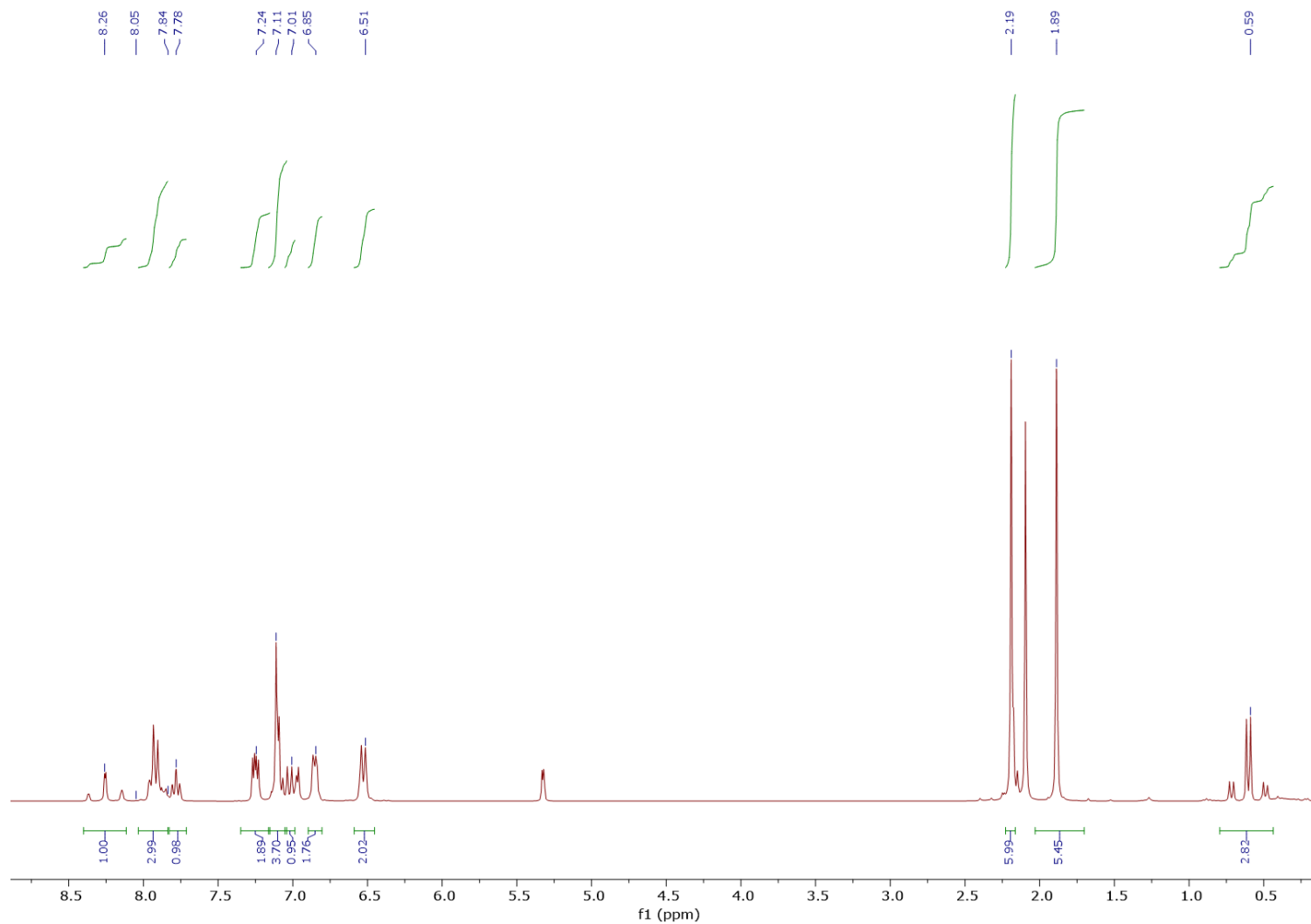
Figura S10. ^{1}H NMR spectrum of complex of **1·CO** in CD$_2$Cl$_2$.

173.80
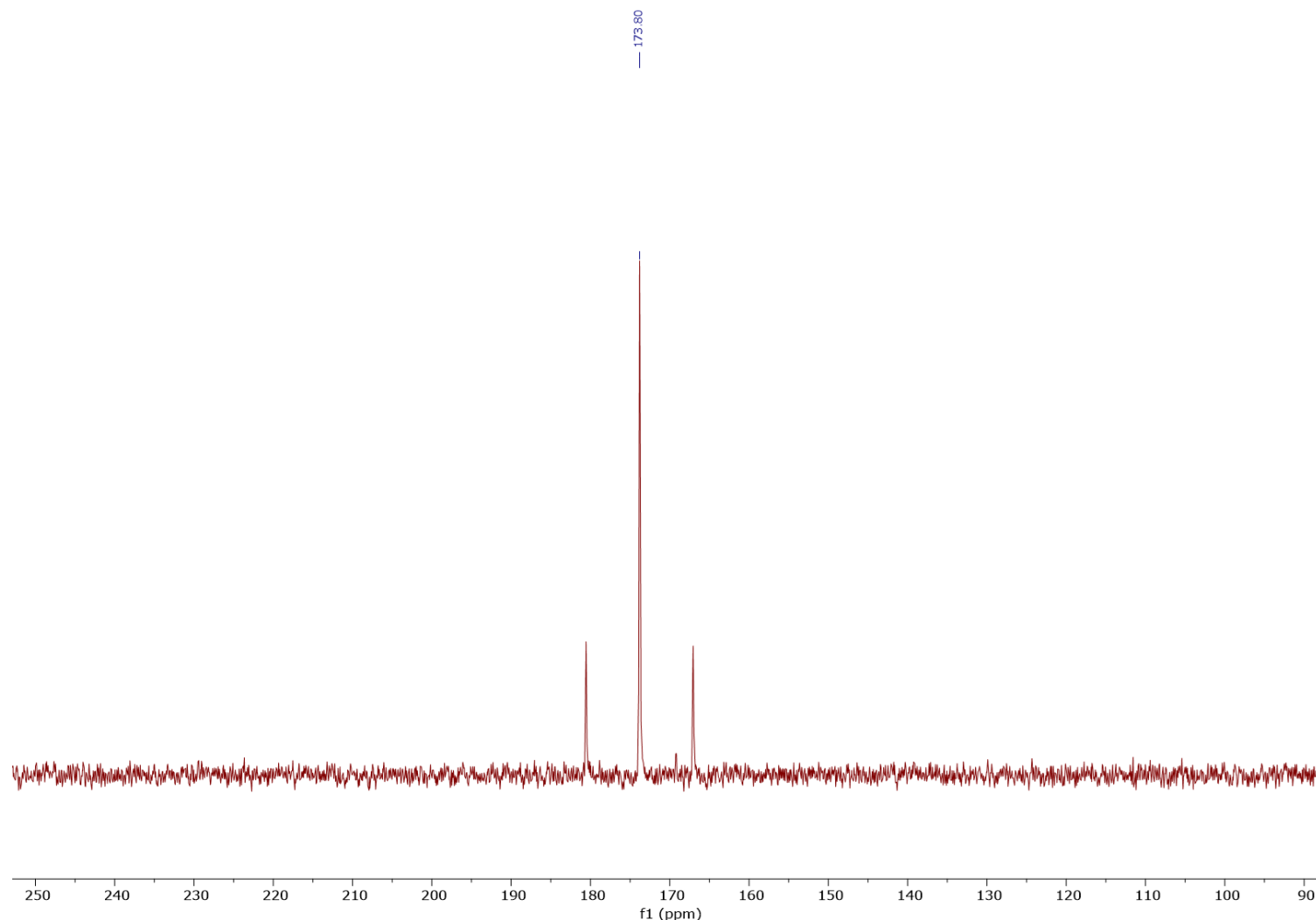
Figura S11. $^{31}P\{^{1}H\}$ NMR spectrum of complex of **1·CO** in CD$_2$Cl$_2$.
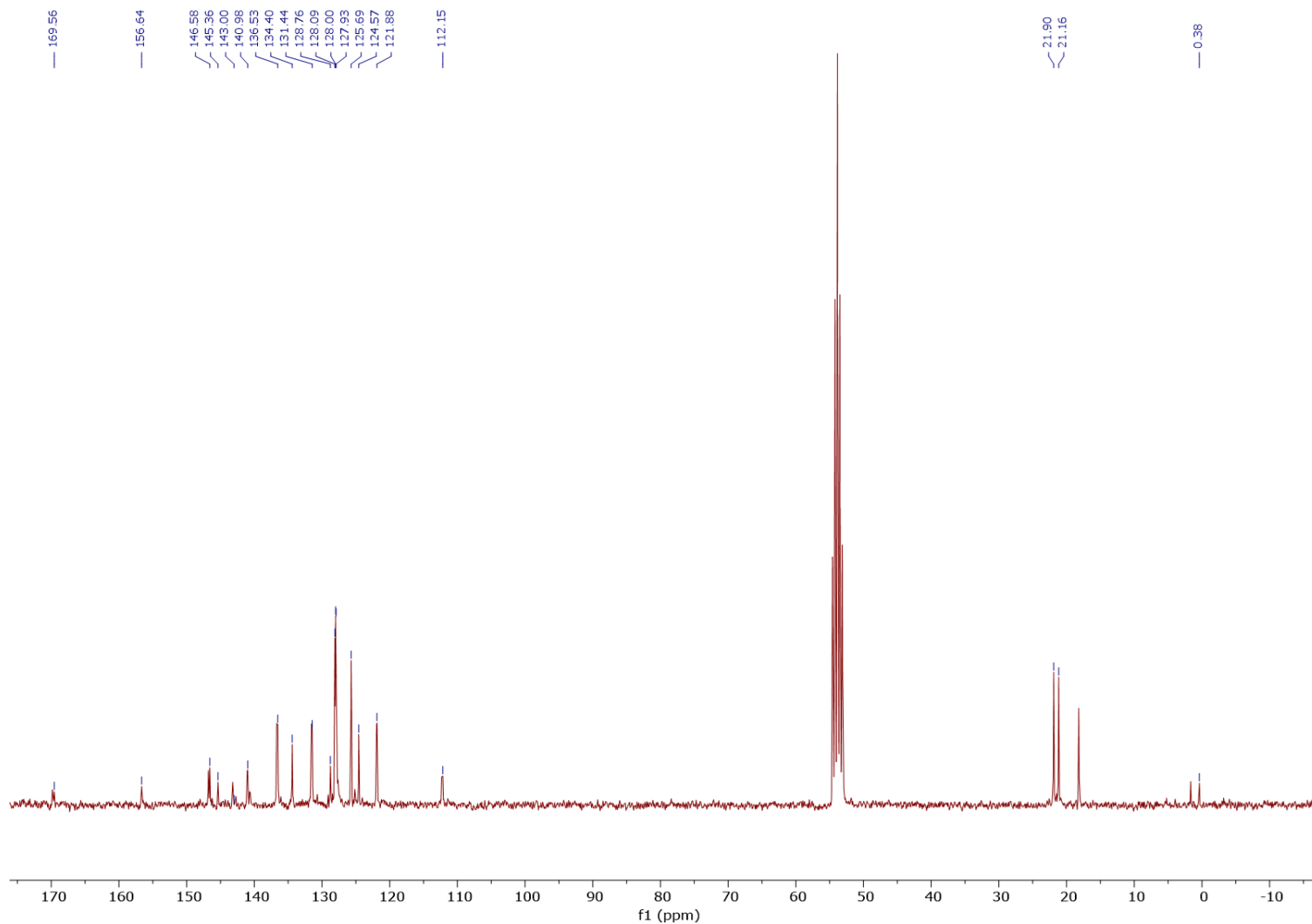
Figura S12. $^{13}C\{^{1}H\}$ NMR spectrum of complex of **1·CO** in CD_2Cl_2.
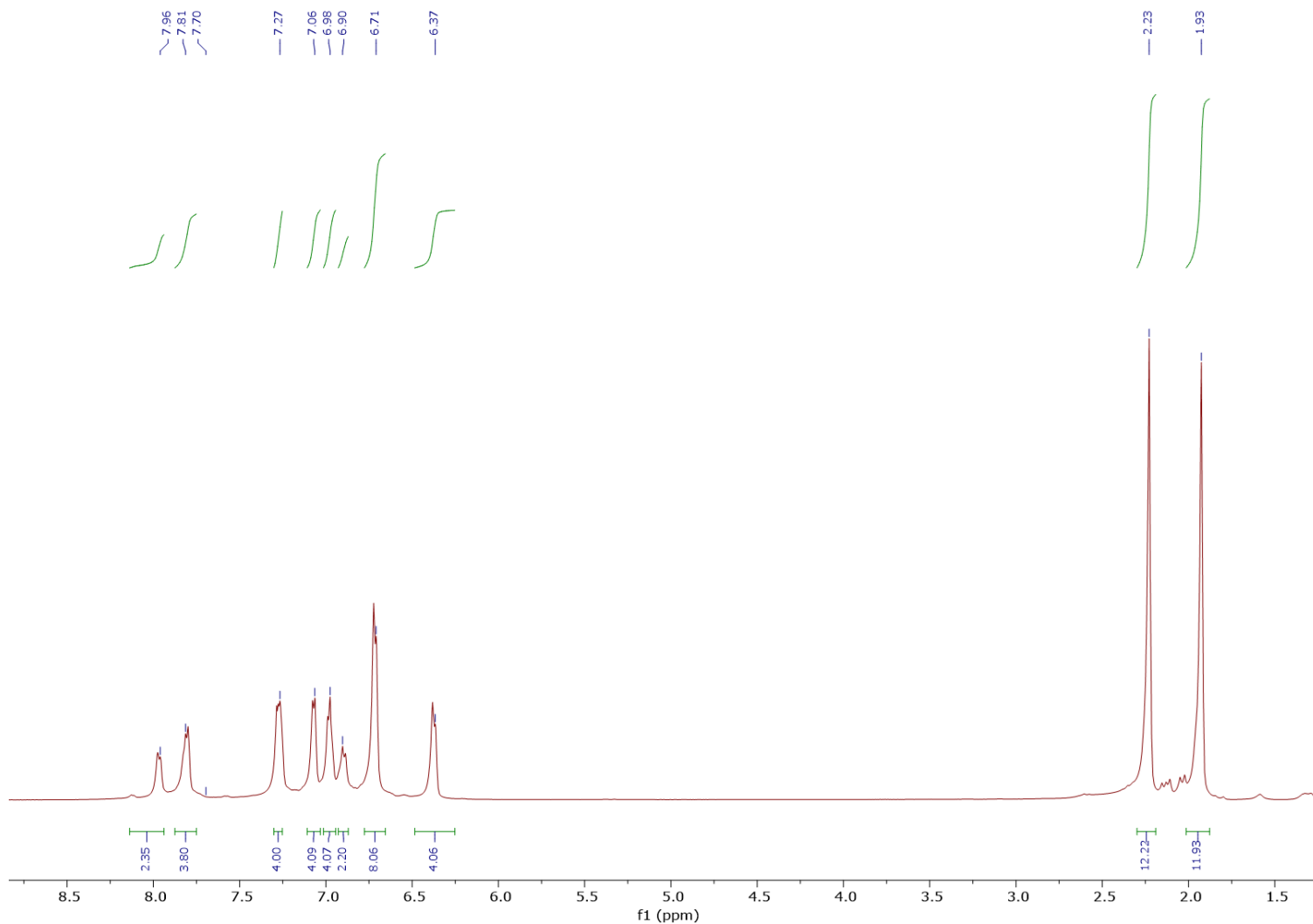
Figura S13. ^{1}H NMR spectrum of complex of **2** in CDCl$_3$.
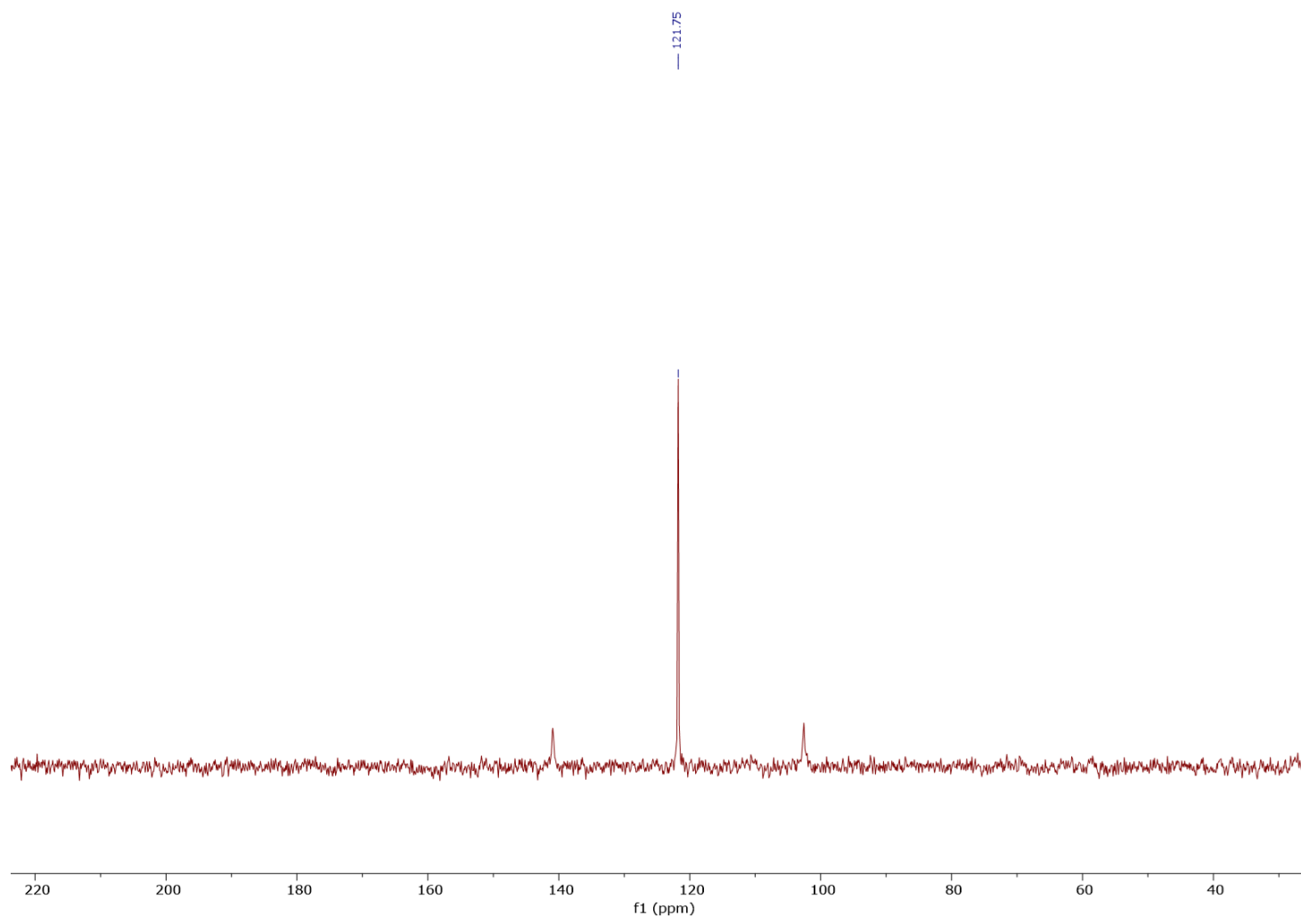
Figura S14. $^{31}P\{^{1}H\}$ NMR spectrum of complex of **2** in CDCl$_3$.
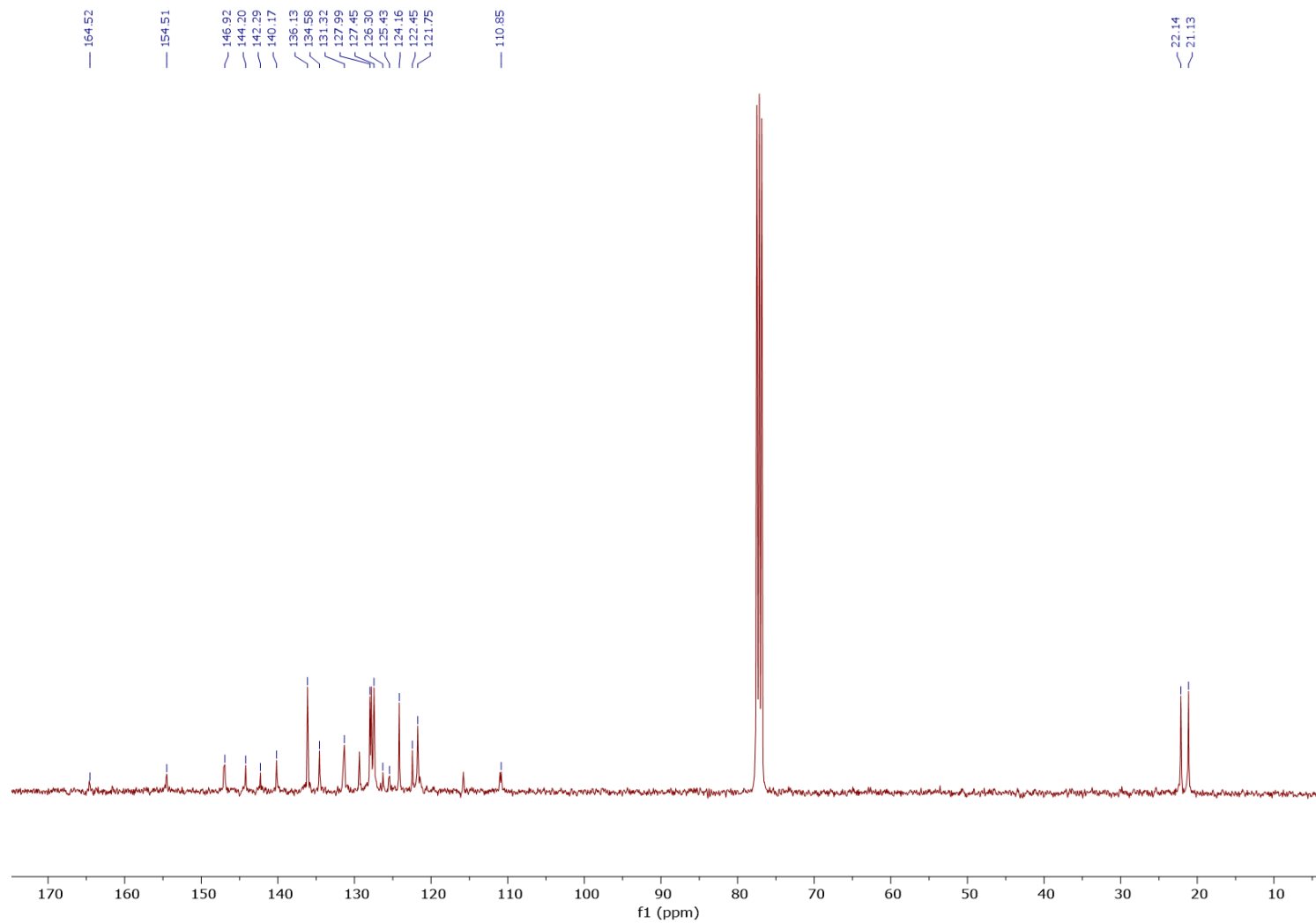
Figura S15. $^{13}C\{^1H\}$ NMR spectrum of complex of **2** in CDCl$_3$.
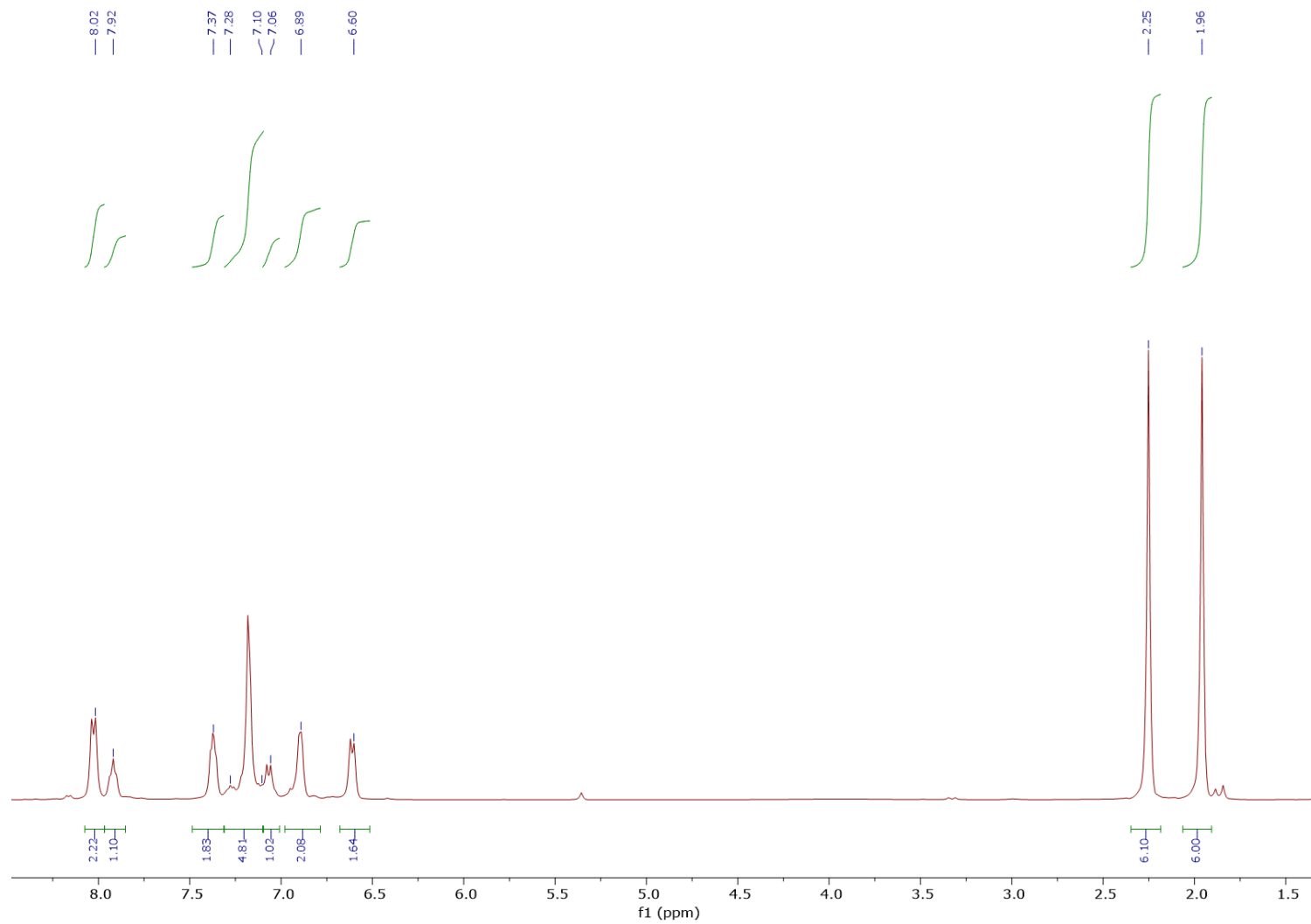
Figura S16. ¹H NMR spectrum of complex of **2·CO** in CD₂Cl₂.

132.56
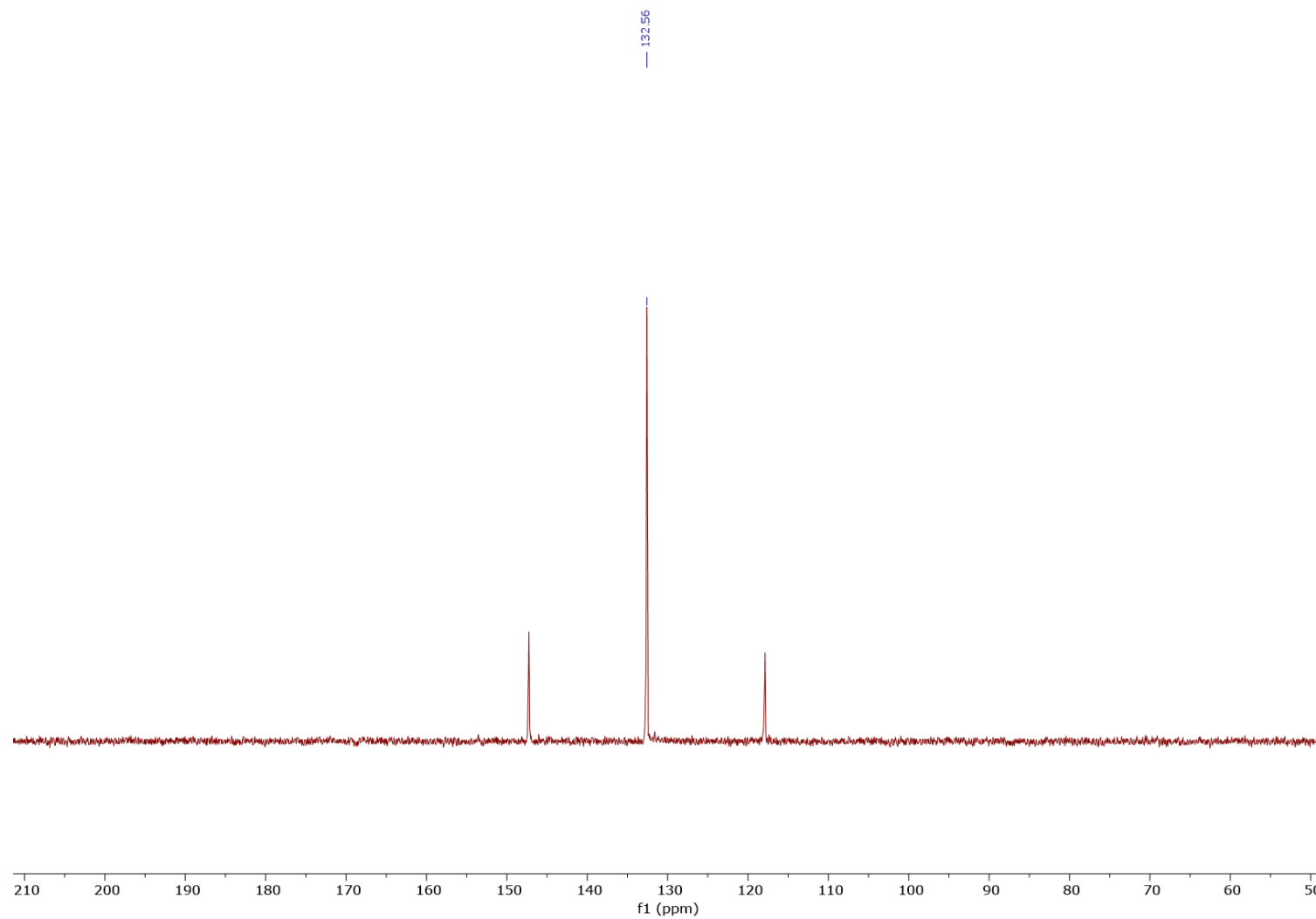
Figura S17. $^{31}P\{^{1}H\}$ NMR spectrum of complex of **2·CO** in CD_2Cl_2.
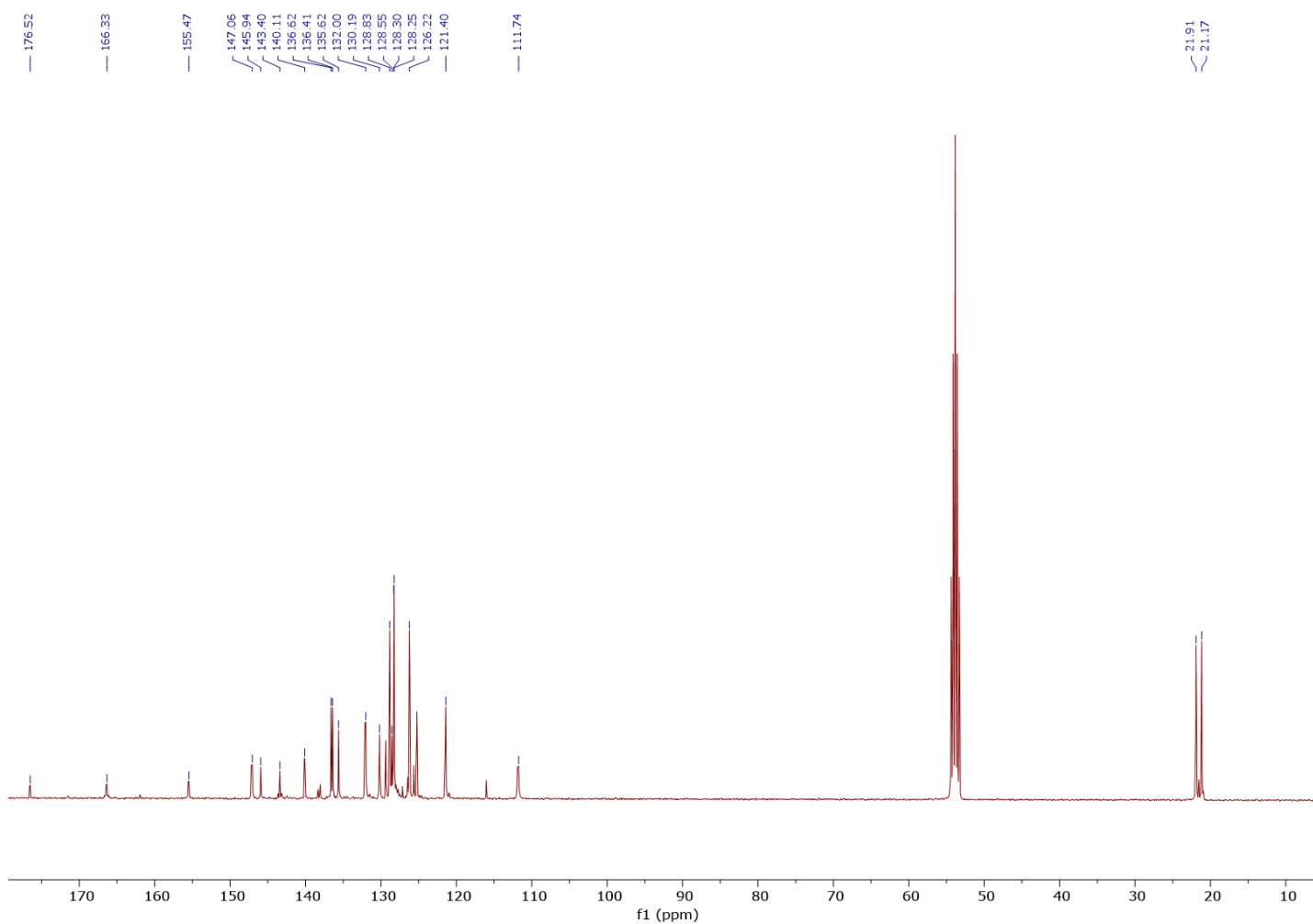
Figura S18. $^{13}C\{^1H\}$ NMR spectrum of complex of **2·CO** in CD_2Cl_2.
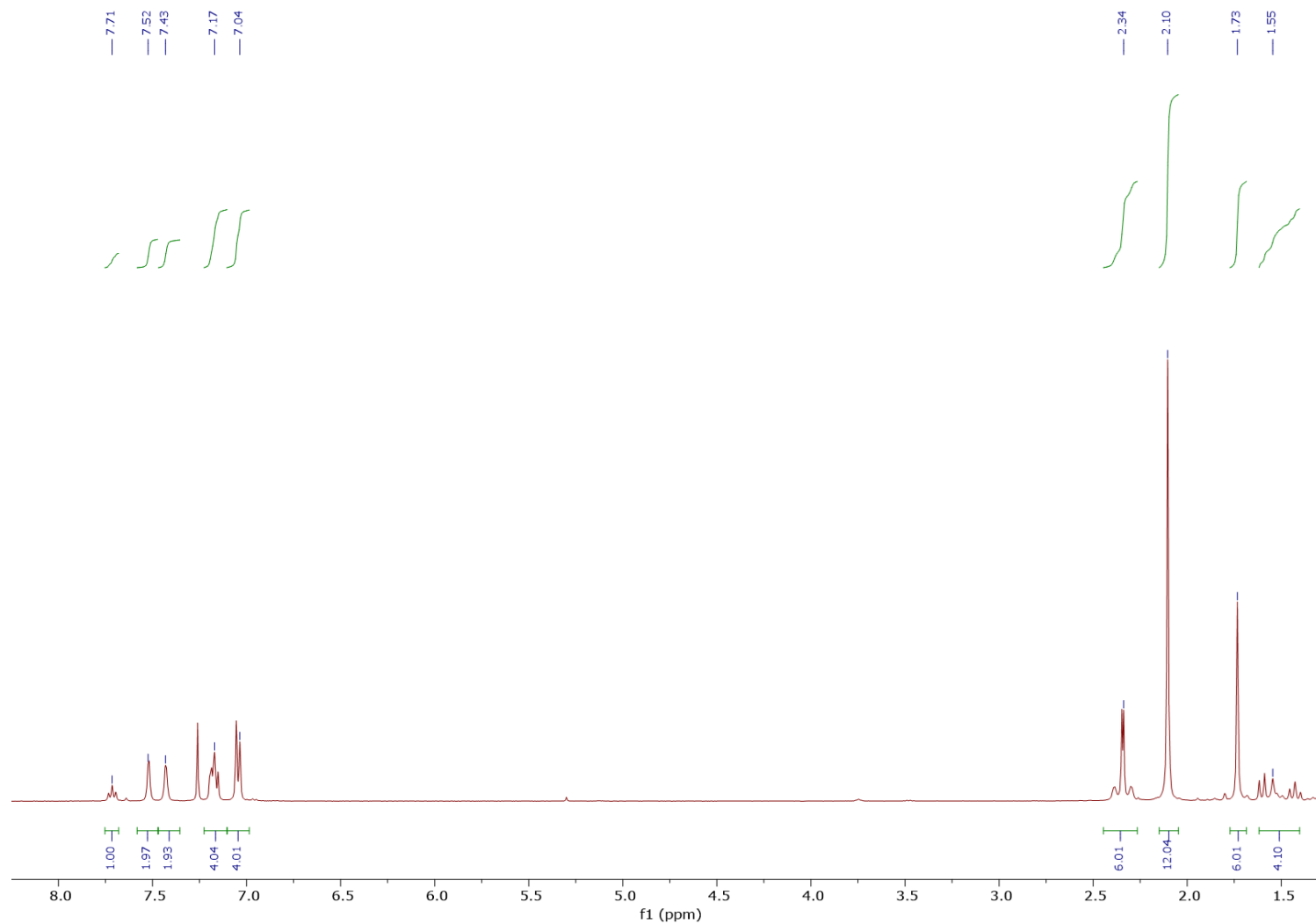
Figura S19. ^{1}H NMR spectrum of complex of **3·SMe₂** in CDCl₃.

165.59
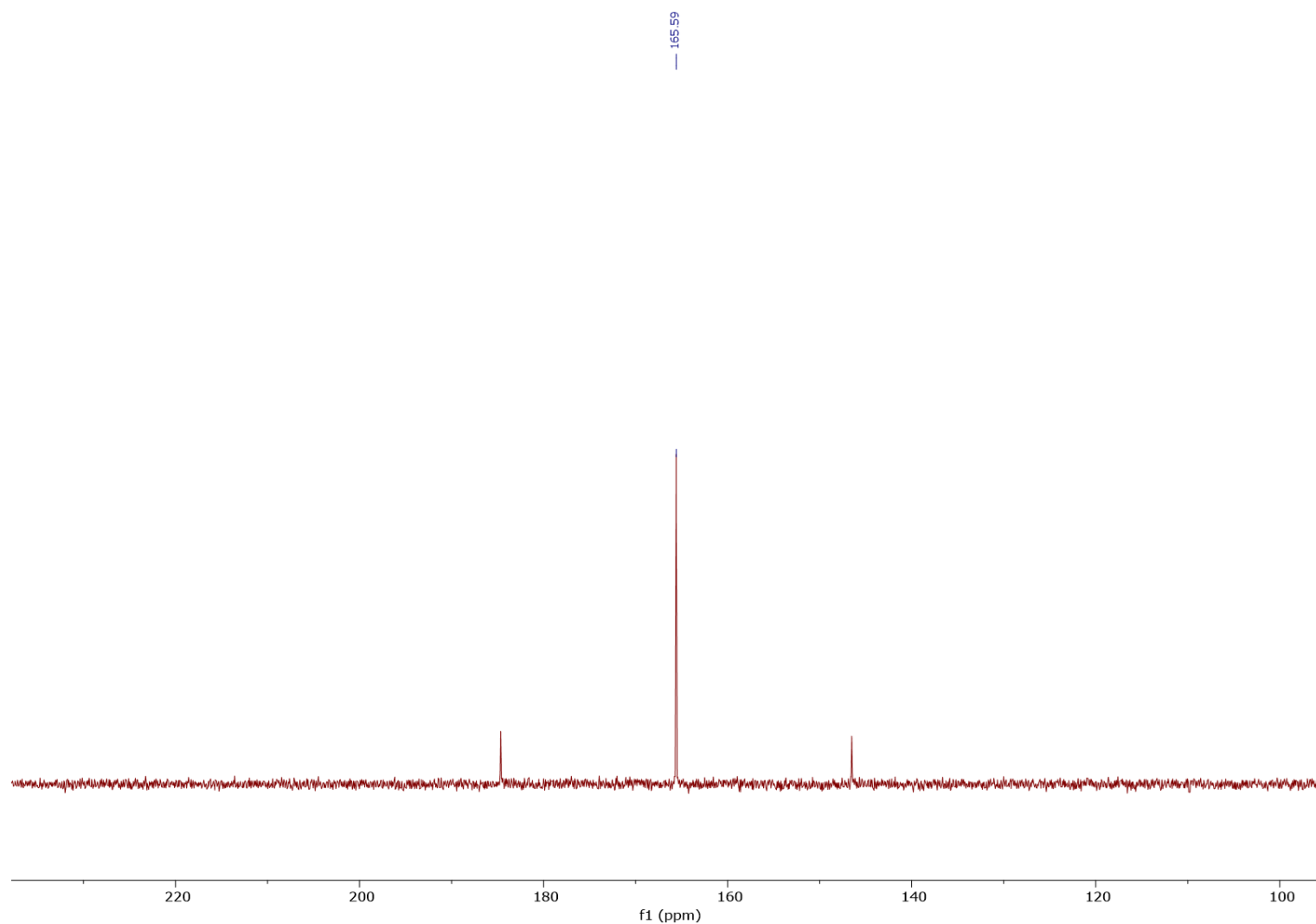
Figura S20. $^{31}P\{^1H\}$ NMR spectrum of complex of **3·SMe$_2$** in CDCl$_3$.
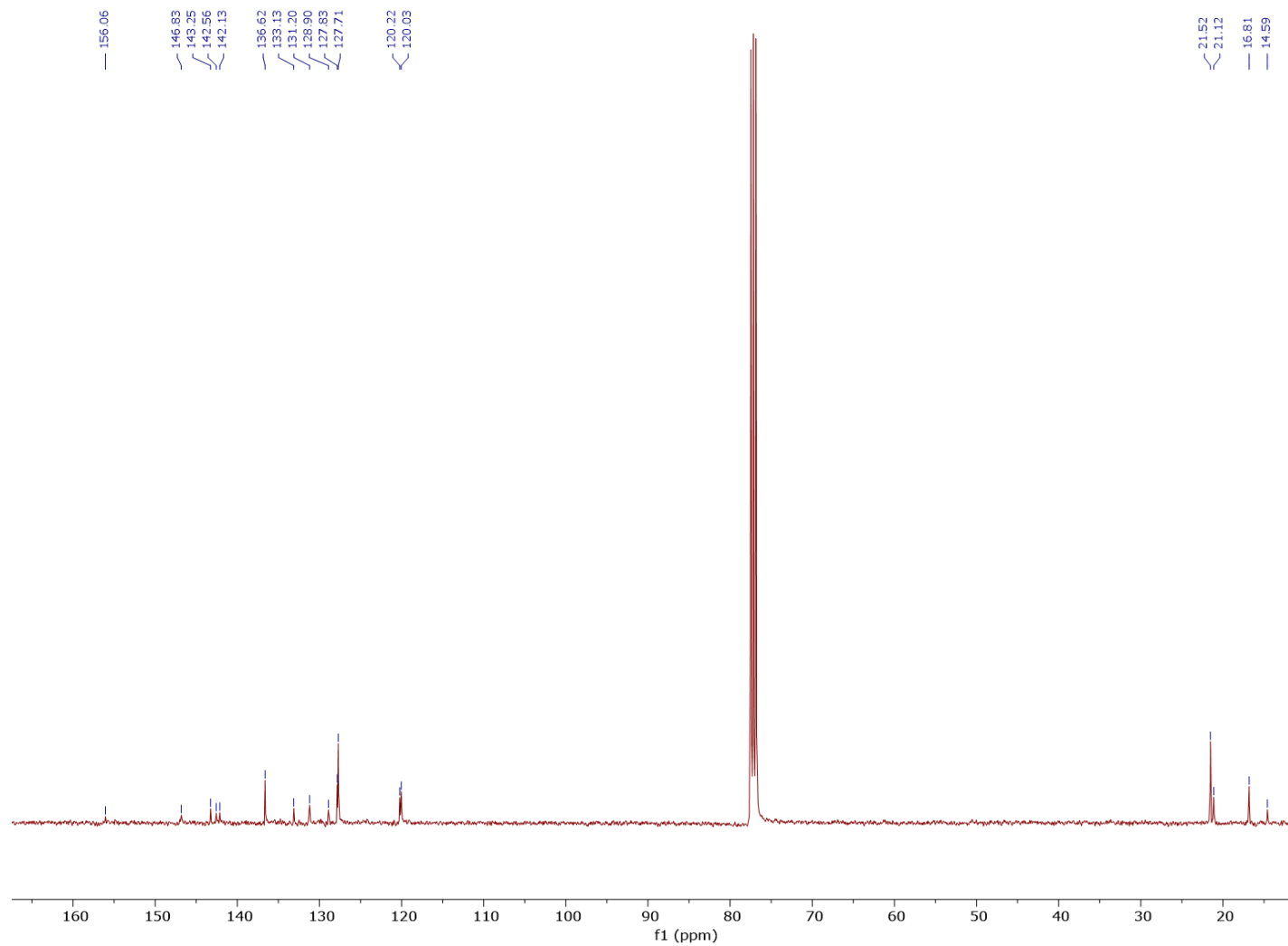
Figura S21. $^{13}C\{^1H\}$ NMR spectrum of complex of **3·SMe₂** in CDCl₃.
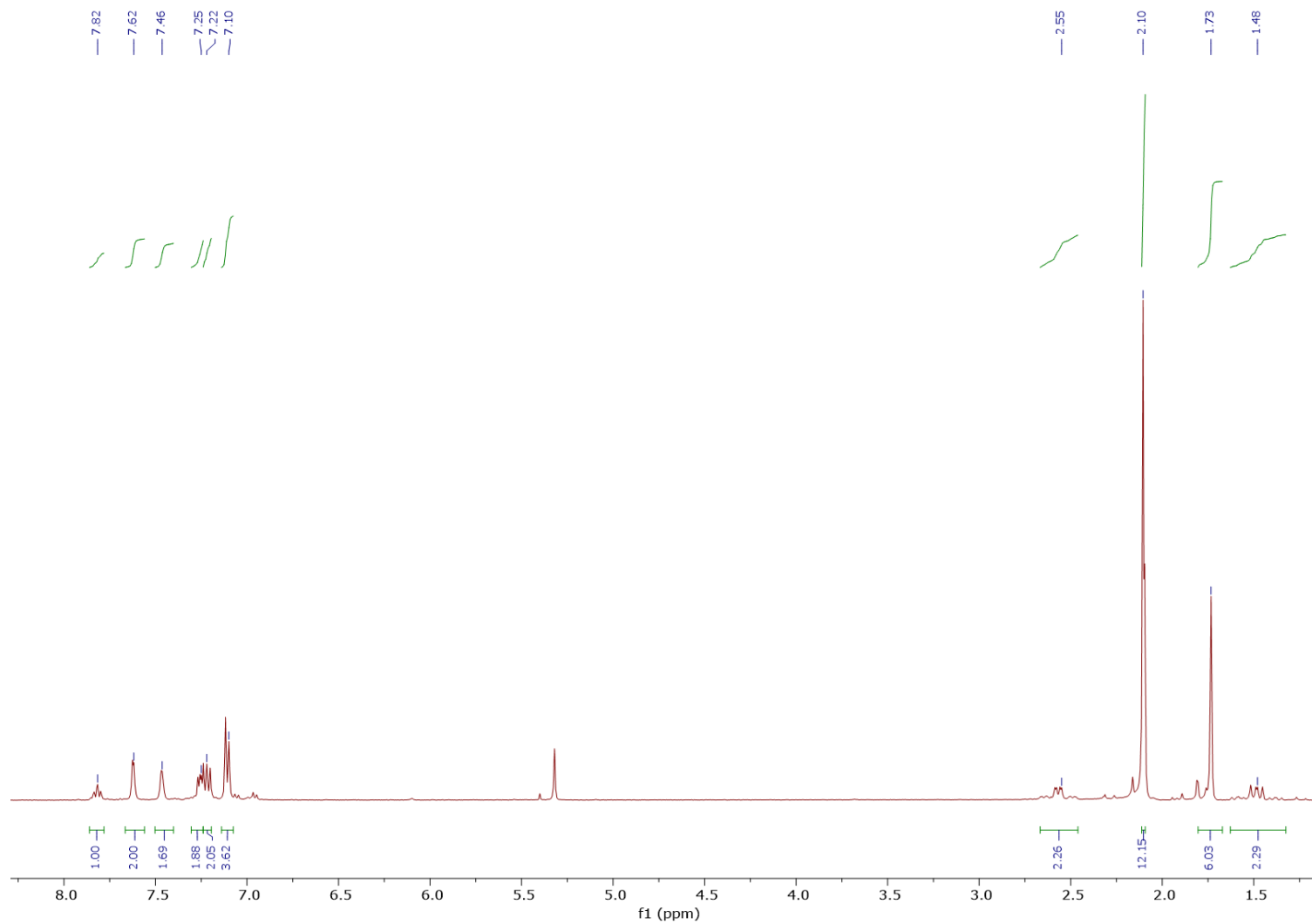
Figura S22. ^{1}H NMR spectrum of complex of **3·CO** in CD_2Cl_2.
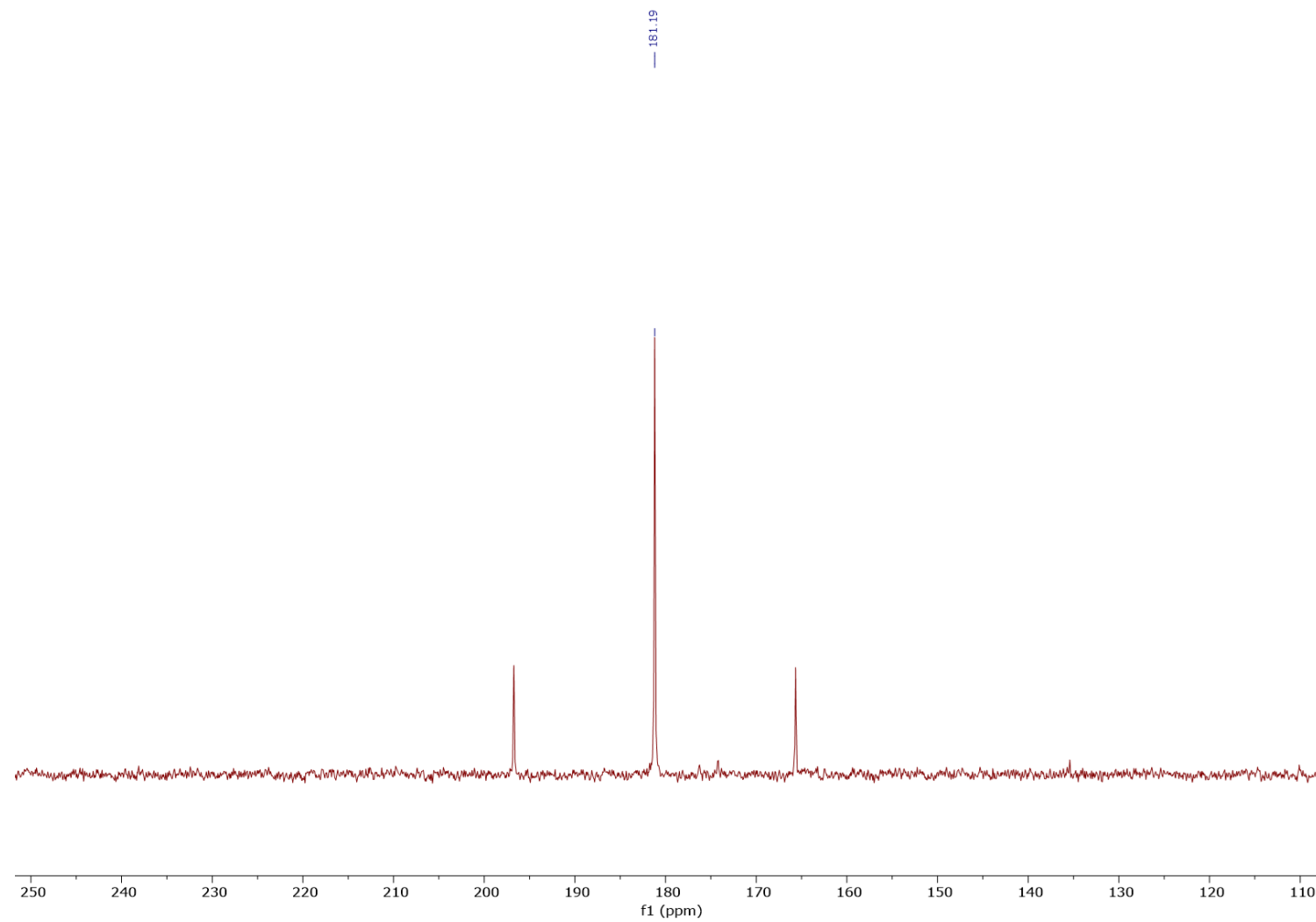
Figura S23. $^{31}P\{^{1}H\}$ NMR spectrum of complex of **3·CO** in CD$_2$Cl$_2$.
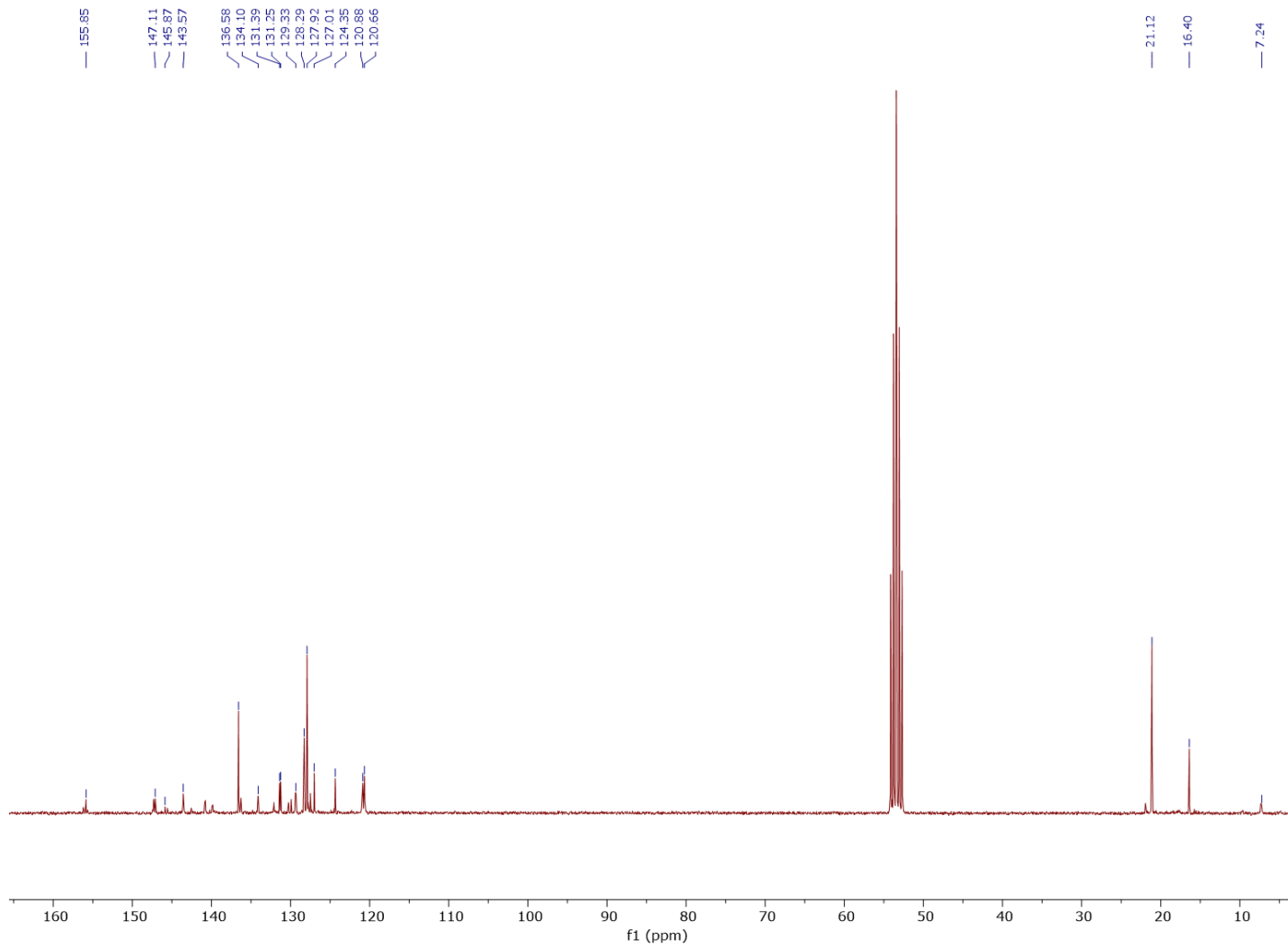
**Figura S24.** $^{13}C\{^1H\}$ NMR spectrum of complex of **3·CO** in CD_2Cl_2.
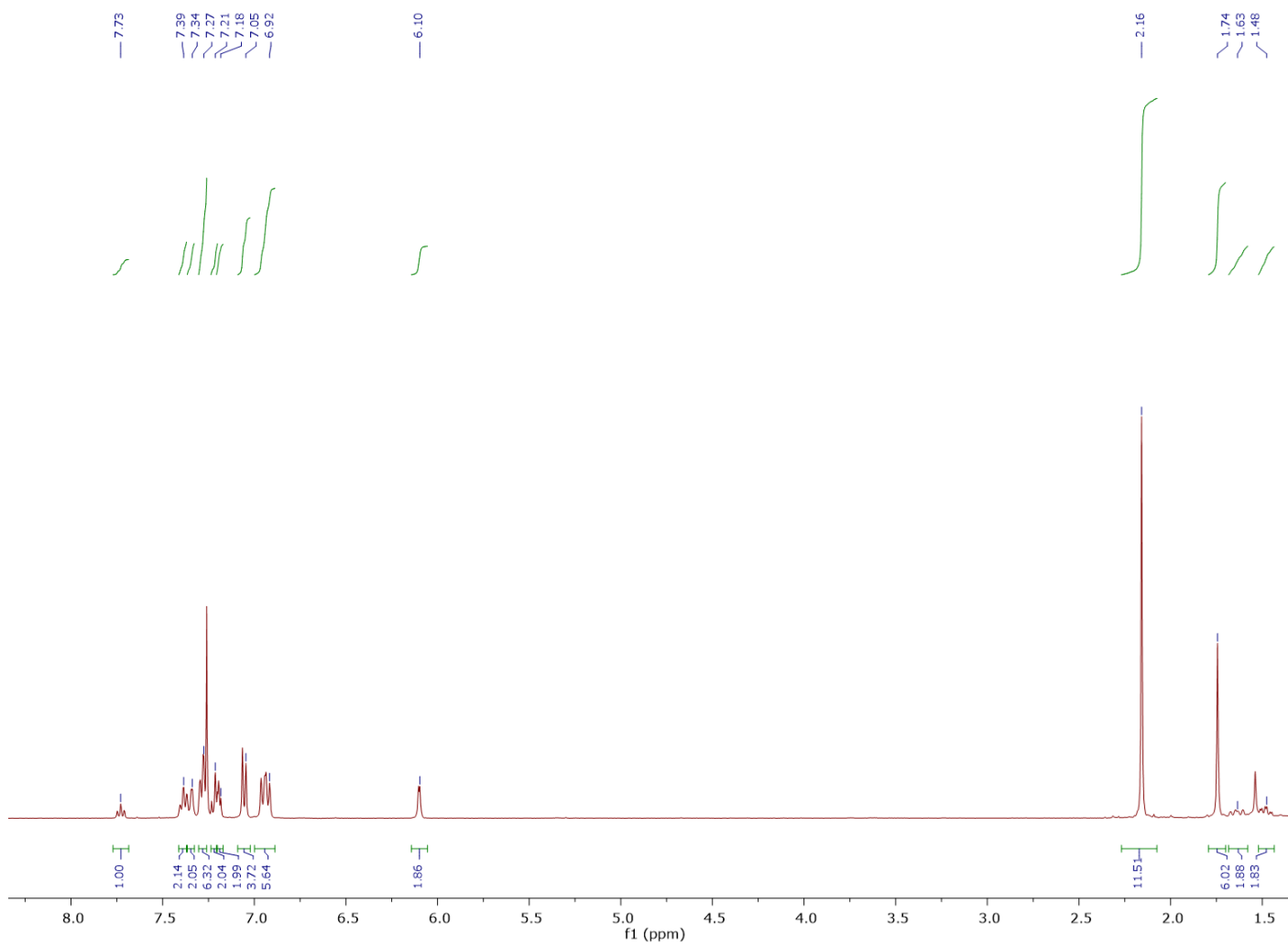
Figura S25. ^{1}H NMR spectrum of complex of **3·PPh₃** in CDCl₃.
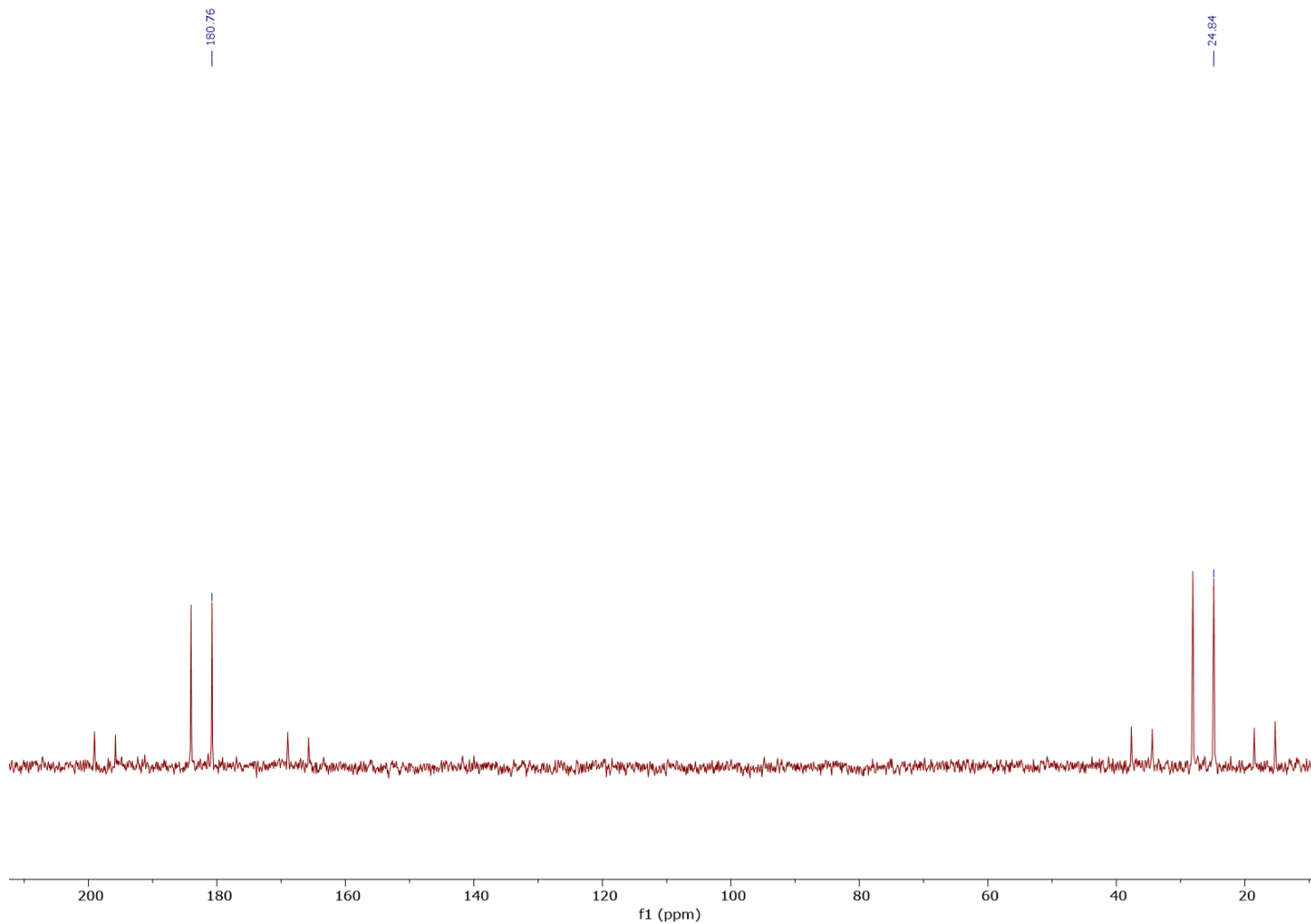
**Figura S26.** ^{31}P{^{1}H} NMR spectrum of complex of **3·PPh₃** in CDCl₃.
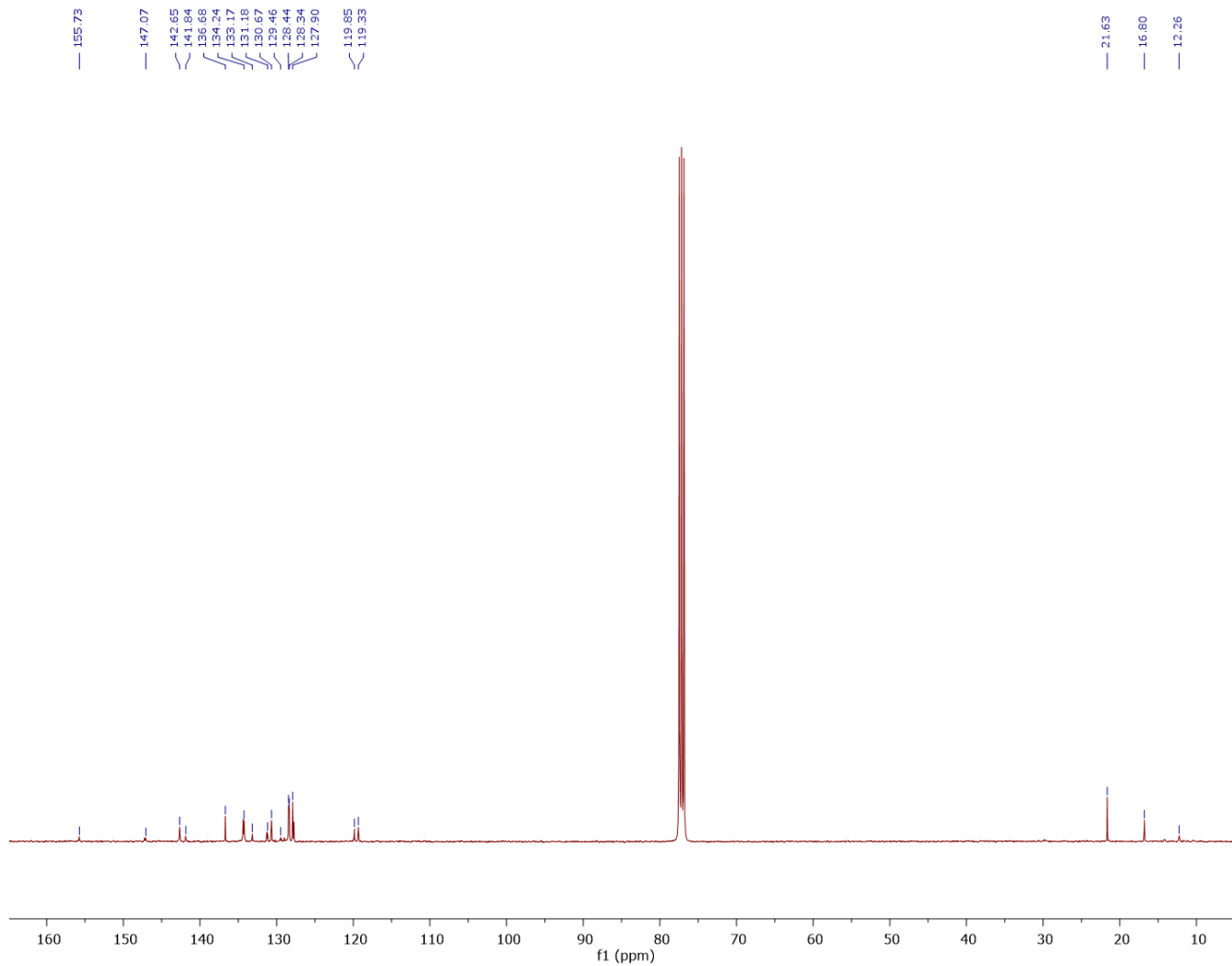
Figura S27. $^{13}C\{^{1}H\}$ NMR spectrum of complex of **3·PPh₃** in CDCl₃.